

Structure and photochemistry of a novel tetrazole-saccharyl conjugate isolated in solid argon

A. Ismael^a, A. Borba^b, L. Duarte^b, B.M. Giuliano^b, A. Gómez-Zavaglia^{b,c,*}, M.L.S. Cristiano^{a,*}

^aCCMAR and Department of Chemistry and Pharmacy, FCT, University of Algarve, P-8005-039 Faro, Portugal

^bDepartment of Chemistry, University of Coimbra, P-3004-535 Coimbra, Portugal

^cCenter for Research and Development in Food Cryotechnology (CIDCA), La Plata, Argentina

HIGHLIGHTS

- ▶ A novel tetrazole-saccharyl conjugate (1-TE-BZT) was synthesised.
- ▶ 1-TE-BZT was isolated in argon matrices.
- ▶ The photochemistry of 1-TE-BZT was investigated.
- ▶ Three photofragmentation pathways involving both the cleavage of the tetrazole and the saccharyl moieties were proposed.
- ▶ On the basis of quantum chemical calculations, the proposed photoproducts could be assigned.

ARTICLE INFO

Article history:

Available online 8 May 2012

Keywords:

Saccharin
Tetrazole
Molecular structure
Matrix isolation
Photochemistry

ABSTRACT

A combined matrix isolation FTIR and theoretical DFT/B3LYP/6-311++G(3df,3pd) study of the novel synthesised tetrazole-saccharyl conjugate 2-[1-(1H-tetrazol-5-yl)ethyl]-1,2-benzisothiazol-3(2H)-one 1,1-dioxide [1-TE-BZT] was performed. In the gas phase, at room temperature, the compound exists as a mixture of six isomeric forms (four conformers of 1H tautomer and two conformers of 2H tautomer). According to theoretical calculations, conformers 1H were the most stable and the relative energies among the three most stable forms are lower than 4 kJ mol⁻¹. These conformers benefit from stabilising intramolecular hydrogen bonds-like interactions involving the 1H of the tetrazole ring and the carbonyl oxygen of the saccharyl moiety.

The photochemistry of 1-TE-BZT in solid argon was investigated and theoretical DFT/B3LYP/6-311++G(3df,3pd) calculations also helped in assignment of the experimental bands. A quick consumption of the compound occurred after irradiation of the matrix with UV laser light at $\lambda = 275$ nm. Three photofragmentation pathways were proposed, one leading to 2-[1-(1H-diaziren-3-yl)ethyl]-1,2-benzisothiazol-3(2H)-one 1,1-dioxide and molecular nitrogen, a second one giving 2-(1,1-dioxide-3-oxo-1,2-benzisothiazol-2(3H)-yl)propanenitrile and azide, and a third one involving loss of azide from the tetrazole ring and decarbonylation of the saccharyl ring of 1-TE-BZT to give acrylonitrile and 7-thia-8-azabicyclo[4.2.0] octa-1,3,5-triene 7,7 dioxide. The comparison of the relative intensities of the bands of the photoproducts obtained from the three channels allowed us to consider the latter pathway, involving an unprecedented photocleavage of the benzisothiazole (saccharyl) ring, as the preferred photodegradation channel of 1-TE-BZT.

© 2012 Elsevier B.V. All rights reserved.

1. Introduction

Tetrazoles and benzisothiazoles are nitrogen heterocycles with important applications in major areas, such as medicine, agriculture, imaging technology and food chemistry. In the case of

tetrazoles, most of the applications derive from the acid/base properties of the tetrazolic acid fragment, —CN₄H, which acts as a metabolically stable surrogate for the carboxylic acid group [1]. These compounds can find wide applications in coordination chemistry, as ligands. It has been demonstrated that the heterocycle tetrazole is able to participate in at least nine distinct types of coordination modes with metal ions, in the construction of novel metal-organic frameworks. Furthermore, the coordination ability of the tetrazolyl ligand through four nitrogen electron-donating atoms allows it to serve as a bridging building block in supramolecular assemblies.

* Corresponding authors. Address: Center for Research and Development in Food Cryotechnology, La Plata, RA 1900, Argentina. (A. Gómez-Zavaglia).

E-mail addresses: angoza@qui.uc.pt (A. Gómez-Zavaglia), mcristi@ualg.pt (M.L.S. Cristiano).

1,2-Benzisothiazole-3-one 1,1-dioxide anions (deprotonated saccharines), also interact with metal centres, mostly through hydrogen bonding [2,3].

Tetrazolyl and saccharyl ethers have particularly important synthetic uses as intermediate compounds for reductive cleavage of the C–O bond in allyl- benzyl- and naphthyl alcohols and phenols catalysed by transition metals [4–7]. Much of the reactivity of these ethers is ascribed to changes in bond lengths around the central C_{HAR}–O–C_A ether bonds (HAR = heteroaromatic ring and A = alkyl allyl, benzyl, phenyl or naphthyl group), caused by the powerful electron-withdrawing effect of the benzisothiazole ring system. The neat result of these electronic changes determines a molecular structure in which the originally strong C_A–O bond in the alcohol or phenol lengthens becoming easily cleavable in the ether whereas the CH_{AR}–O bond acquires a considerable degree of double bond character. As such, thermal treatment of these compounds leads to easy cleavage of the C_A–O bond together with the formation of a C_{HAR}=O bond [8–12]. The thermally induced isomerisation of various allyloxy- and alkoxy-benzisothiazoles was investigated and proved to involve intramolecular migration of the allyl or alkyl groups from O to N and occur through an intramolecular sigmatropic rearrangement.

Considering the wide interest demonstrated in tetrazole and benzisothiazole heterocycles as multidentate nitrogen ligands [13,14], efforts were made to prepare tetrazole-saccharyl conjugates with various linkers and to investigate their structure and reactivity. Our previous works revealed that the benzisothiazole moiety is photochemically stable whereas tetrazoles are highly photoreactive [14–22]. Thus, combining the apparent photochemical inertness of the benzisothiazole moiety with the high reactivity of the tetrazole moiety appeared to us as a challenge for this investigation. If the benzisothiazole moiety proves photochemically inert upon photolysis, then new saccharyl derivatives resulting from photolysis of the tetrazole ring may be produced. Alternatively, if conditions for photocleavage of the benzisothiazole moiety are established, photolysis of the tetrazole-saccharyl conjugate will probably produce a set of new compounds, opening ways for the development of synthetic pathways to new scaffolds. Also, to the best of our knowledge the available information related to the photochemistry of benzisothiazoles is still very scarce and all published data report photochemistry in solution [23–26]. This scenario prompted us to explore the photolysis of the benzisothiazolyl-tetrazole conjugate by matrix isolation FTIR spectroscopy. The fact that in a cryogenic inert matrix the photochemical processes are cage-confined (molecular diffusion is inhibited) introduces a useful simplification to the study of the photochemical reactivity since no cross reactions can, in principle, take place and only primary unimolecular reactions are expected. Such

simplification is very useful for mechanistic elucidations and for the study of intermediates that are unstable at room temperature but that can be trapped in the matrices. Therefore, in this paper we describe the structure and scrutinise the photochemistry of a novel alkyl-linked tetrazole-saccharyl conjugate, 2-[1-(1*H*-tetrazol-5-yl)ethyl]-1,2-benzisothiazol-3(2*H*)-one (1-TE-BZT), isolated in solid argon. The experimental results are supported by quantum chemical calculations undertaken at the DFT(B3LYP)/6-311++G(3df,3pd) level of theory. As detailed below, unprecedented information concerning the matrix photochemistry of this tetrazole-saccharyl system was gathered.

2. Experimental and computational methods

2.1. Synthesis

The synthetic route to 2-[1-(1*H*-tetrazol-5-yl)ethyl]-1,2-benzisothiazol-3(2*H*)-one 1,1-dioxide (1-TE-BZT) is presented in Fig. 1. Experimental details for the compounds prepared are as follows.

2.1.1. 1-(1*H*-tetrazol-5-yl)ethanol, 2

Prepared from sodium azide (1.43 g; 22 mmol), zinc bromide (4.50 g; 20 mmol) and 2-hydroxy-propanenitrile **1** (1.45 mL; 20 mmol), in water (50 mL). The reaction mixture was refluxed for 20 h with vigorous stirring. White amorphous powder (1.70 g; 75% yield). IR ν_{\max} (cm⁻¹): 3390 (OH), 1696, 1624, 1243, 1123; ¹H NMR (CDCl₃): δ 7.55 (br, 1H), 7.22–7.35 (q, 1H), 7.35 (d, 3H); MS (EI), *m/z* 115 (33%) [M+H]⁺, 1 *m/z* 132 (100%) [M+NH₄]⁺. Acc. Mass (CI): found, 115.1145; calcd. for C₃H₇N₄O, 115.1134.

2.1.2. 3-Chloro-1,2-benzisothiazole 1,1-dioxide, 3

Prepared from saccharin (10.2 g; 56 mmol), and phosphorus pentachloride (14.0 g; 66 mmol) heated at 180 °C. Colourless needles from trichloromethane (7.00 g; 63% yield), m.p. 143–145 °C. IR ν_{\max} : 1724, 1654, 1603 (C=C), 1346 (SO₂), 775 (Ar–H) and 692 (C–Cl) cm⁻¹; ¹H NMR (CDCl₃): δ 7.85 (4H, m, Ar–H); Anal. calcd. for C₇H₄NO₂Cl: C, 41.7; H, 2.0; N, 7.0%, found: C, 41.5; H, 2.0; N, 6.9%; MS (EI), *m/z* 201 [M]⁺.

2.1.3. 2-[1-(1*H*-tetrazol-5-yl)ethyl]-1,2-benzisothiazol-3(2*H*)-one 1,1-dioxide 5

A mixture of 1-(1*H*-tetrazol-5-yl)ethanol **2** (0.20 g; 1.75 mmol), 3-chloro-1,2-benzisothiazole 1,1-dioxide (0.35 g; 1.75 mmol) and potassium tert-butoxide (0.65 g; 5.25 mmol, in dry THF (50 mL), was stirred at 60 °C under a nitrogen atmosphere, until TLC analysis (DCM/toluene 3:1) indicated the absence of starting material (48 h). Work-up afforded a pale yellow powder (0.28 g; 58% yield), m.p. 210–211 °C identified as 1-TE-BZT, **5**. IR ν_{\max} : 3091, 2974, 1721, 1593, 1463, 1336 (SO₂), 1177 cm⁻¹; ¹H NMR (CDCl₃): δ 8.05–8.08 (d, 1H), 7.91–7.95 (m, 2H), 7.86–7.90 (d, 1H), 5.26 (1H, d), 1.39–1.41 (d, 3H); MS (EI), *m/z* 279 [M]⁺; Acc. Mass (CI): found = 280.1089, calcd. for C₁₀H₁₀N₅O₃S: 280.1022.

2.2. Infrared spectroscopy and photochemical experiments

The infrared (IR) spectra of 1-TE-BZT were obtained using a Nicolet 6700 Fourier transform infrared spectrometer equipped with a deuterated triglycine sulphate (DTGS) detector and a Ge/KBr beam splitter, with 0.5 cm⁻¹ spectral resolution. Matrices were prepared by co-deposition, onto the cooled CsI substrate of the cryostat, of the matrix gas (argon 99.9998%, obtained from Air Liquide) and vapours of the compound under study produced by evaporation in a specially designed temperature variable mini-oven assembled inside the cryostat. The temperature of the

Table 1

Zero point corrected relative energies (ΔE_0 /kJ mol⁻¹) obtained at the DFT(B3LYP)/6-311++G(3df,3pd) level of theory of the various conformers of 1-TE-BZT^a and average energies ($-\Delta H$ /kJ mol⁻¹) for intramolecular interactions involving the NH group in 1*H* conformers of 1-TE-BZT, calculated using equations 1 and 2 (see text).^b

Tautomer	Conformer	ΔE_0 DFT(B3LYP)/6-311++G(3df,3pd)	NH...O=X (nm)	$\Delta\nu_{\text{NH}}$ (cm ⁻¹)	$-\Delta H$ (kJ mol ⁻¹)
1 <i>H</i>	G'Sk'	0.0 (-3370201.670) ^c	0.2047	175.4	16.1
	GSK'	2.59	0.2012	194.5	17.2
	G'Sk	4.25	0.2150	129.8	13.1
	GSK	8.30	0.2179	119.8	12.4
2 <i>H</i>	G'G'	7.12			
	GG'	8.60			

^a Energies in kJ mol⁻¹; conformers are depicted in Fig. 3.

^b See Fig. 1 for atom numbering.

^c Total energies with zero point vibrational energy contribution.

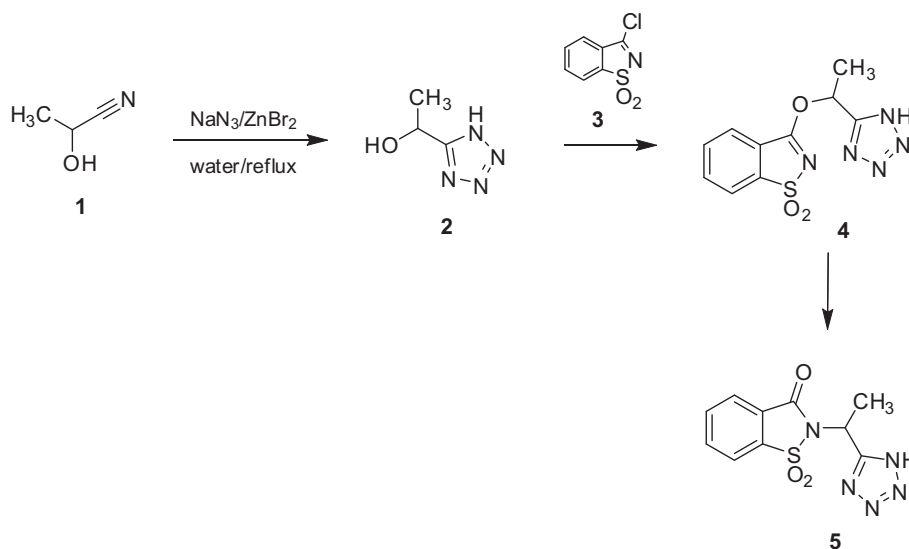


Fig. 1. Synthetic approach to 2-[1-(1H-tetrazol-5-yl)ethyl]-1,2-benzisothiazol-3(2H)-one 1,1-dioxide.

mini-oven used for evaporation of the compounds was *ca.* 335 K. The low temperature experiments were done on the basis of an APD Cryogenics close-cycle helium refrigeration system with a DE-202A expander. The temperature of the CsI substrate during deposition was 15 K.

The matrices were irradiated through the outer quartz window of the cryostat, with the frequency-doubled signal beam of the Quanta-Ray MOPO-SL pulsed (10 ns) optical parametric oscillator (FWHM $\sim 0.2\text{ cm}^{-1}$, repetition rate 10 Hz, pulse energy $\sim 2.5\text{ mJ}$) pumped with a pulsed Nd:YAG laser.

2.3. Computational methods

The quantum chemical calculations were performed at the DFT level of theory using the standard 6-311++G(3df,3pd) basis set [27–31] and the three-parameter density functional abbreviated as B3LYP, which includes Becke's gradient exchange correction [32] and the Lee, Yang, Parr correlation functional [33]. Geometrical parameters were optimised using the Direct Inversion in the Iterative Subspace (DIIS) method [34]. The optimisation of geometries was followed by harmonic frequency calculation at the same theory level. The nature of the obtained stationary points was checked through analysis of the corresponding Hessian matrix. Calculations were carried out using the Gamess program [35].

The calculated harmonic frequencies (scaled with the factor 0.978 [14]) were used to assist the analysis of the experimental spectra and to account for the zero-point vibrational energy (ZPVE) corrections.

3. Results and discussion

3.1. Synthesis of 2-[1-(1H-tetrazol-5-yl)ethyl]-1,2-benzisothiazol-3(2H)-one 1,1-dioxide

The synthetic route to 1-TE-BZT is presented in Fig. 1 and involves a convergent strategy whereby the tetrazolyl and saccharyl building blocks, **2** and **3**, are prepared separately and then coupled to form the ethyltetrazole-saccharyl ether **4** that subsequently isomerises to the required target compound **5**. Sigmatropic isomerisation in saccharyl ethers has been studied by our groups. An earlier investigation of the thermal isomerisation of allyl-saccharyl ethers in solution, revealed that migration of the allyl group from O to N

may occur through both [3,3']- and [1,3']-processes [8,10], the relative proportion of isomerisation products depending on structural features of the starting ether such as electron density and steric hindrance on the allylic system, polarity of the reaction medium and temperature. It was also observed that the saccharyl derivative of the cyclic allyl alcohol myrtenol isomerises at room temperature with exclusive formation of the [1,3']-product. This behaviour was interpreted on the basis of steric constraints imposed by the cyclic myrtenyl system, which destabilise the transition state required for concerted [3,3']-migration, preventing its formation [10]. It was further demonstrated that the [3,3']-products undergo inversion to the thermochemically more favourable [1,3']-isomers upon extended heating [8]. It is not clear whether the [1,3']-rearrangement in these ethers occurs through a fragmentation-recombination process or through a pseudo-pericyclic mechanism. Recently, the thermal isomerisation of neat 3-allyloxysaccharin was investigated in the liquid phase, combining matrix-isolation FTIR spectroscopy, differential scanning calorimetry and quantum chemical calculations. From the results, a [3,3']-sigmatropic shift mechanism for the isomerisation in the liquid phase was proposed [36]. We have also demonstrated that the isomerisation of 3-methoxy-saccharin in the solid-state and in the gas phase occurs through a Chapman-type mechanism [11,12]. Considering this scientific background, it was reasonable to expect that compound **4** would easily isomerise to the target conjugate **5**, and a synthetic approach making use of this reaction was therefore devised. Furthermore, migration of the alkyl group from O to N in ether **4** was expected to be easier than in the case of 3-methoxy-saccharin due to increased stabilisation of the carbocation-like migrating moiety. In fact, ether **4** could not be isolated because it readily isomerises to conjugate 1-TE-BZT, **5**, as could be demonstrated by FTIR and NMR (see Section 2.1.3).

3.2. Geometries and energies of 1-TE-BZT

Before the discussion of geometries and energies of 1-TE-BZT, it must be underlined that for compounds containing sulphur–oxygen linkages, such as benzisothiazoles, it is relatively difficult to obtain reliable predictions of their fundamental properties. More specifically, most of the standard computational methods and basis sets have been found unable to correctly predict the values of the S=O bond lengths and of the vibrational frequencies associated with it [37–40]. To overcome this problem, we decided to use

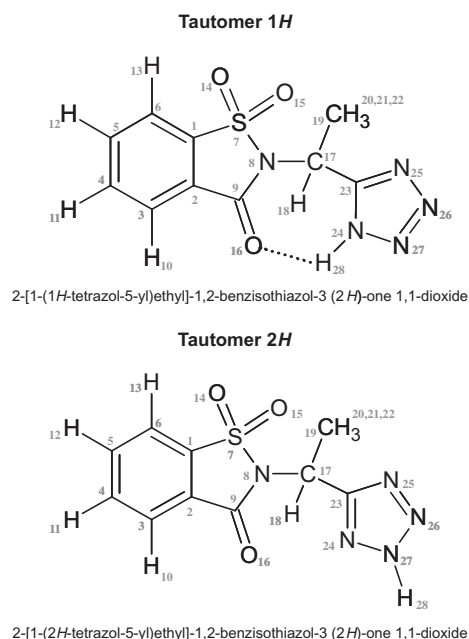


Fig. 2. Schematic representation of the two tautomeric forms of 1-TE-BZT with adopted atom numbering.

the B3LYP functional together with an extensive set of polarisation functions. As demonstrated in our previous work, this approach correctly reproduces both the geometry and frequencies of the hypervalent S=O bonds [41].

1-TE-BZT has a chiral centre, the two enantiomers (R and S forms) being spectroscopically equivalent. In the present study we will focus on the R form. The compound may exist in two tautomeric forms (Fig. 2), both having two conformationally relevant internal degrees of rotation, which are defined by the N₈–C₁₇ and C₁₇–C₂₃ bonds. Other tautomers, such as hydroxy benzisothiazole forms, could, in principle, be considered. These forms involve transfer of H₁₈ to O₁₆ (the carbonyl oxygen in the saccharine ring), forming and imino linkage between both heterocycles (keto–enol tautomerisation). However, taking into account the lower stability of enol forms and considering the high computational efforts required for the optimisation of benzisothiazole derivatives, the enol tautomers have been *a priori* ruled out [16].

The theoretical calculations at the B3LYP/6-311++G(3df,3pd) level predicted a total of six minima on the ground state potential energy surface of 1-TE-BZT. Four minima belong to the conformers of 1H tautomer and the remaining two correspond to the two conformers of 2H tautomer. The full set of conformers found for each tautomer and their calculated relative energies (including zero point energy corrections) are represented in Fig. 3 and Table 1. Geometrical parameters for the various isomers are given in Table S1 (Supporting information). The following systematic rules were used to attribute names to the different isomeric forms: C₉N₈C₁₇C₂₃ is indicated by the first letter (*G* = *gauche*, ca. 60°; *G'* = *gauche'*, ca. –60°); N₈C₁₇C₂₃N₂₄ is indicated by the second letters (*Sk* = *skew*, ca. 120°; *Sk'* = *skew'*, ca. –120° in tautomer 1H and *G'* = *gauche'*, ca. –60° in tautomer 2H). 1H and 2H refer to the position of H₂₈ in the tetrazole ring.

According to calculations, the conformers belonging to the 1H tautomer were found to be the most stable forms. The stabilisation of these forms results from the presence of an intramolecular hydrogen bond-like (NH···O=X, where X = S, C), that is absent in all the 2H conformers. The oxygens acting as electron donors are those bound to C₉ and S₇ of the saccharine ring (O₁₄, O₁₅ and

O₁₆) (see Fig. 1). All 1H conformers are close in energy and the slight energy differences can be understood mainly by considering the distances H₂₈···O=S or H₂₈···O=C. Table 1 shows the theoretically calculated NH···O=X distances for all 1H conformers. Iogensen, Rozenberg and coworkers proposed two empirical Eqs. (1) and (2) allowing the estimation of the hydrogen bond or hydrogen bond-like interaction strengths [42]. The first correlation (1) allows estimating the redshift of the νNH involved in hydrogen bonds or hydrogen bond-like interactions.

$$\Delta\nu\text{NH}/\text{cm}^{-1} = 0.011[r_{\text{H}\cdots\text{H}}/\text{nm}]^{-6.1} \quad (1)$$

where ΔνNH is the redshift induced by the hydrogen bond and $r_{\text{H}\cdots\text{H}}$ is the hydrogen bond distance (NH···O=X in 1-TE-BZT). The second Eq. (2) correlates the redshift estimated in equation 1 with the interaction enthalpy, thus describing the energies of the intramolecular hydrogen bondings involving the NH group of 1H conformers.

$$\Delta H^2 = 1.92 * [\Delta(\nu\text{NH}) - 40] \quad (2)$$

where ΔH is the interaction enthalpy (in kJ mol⁻¹) and ΔνNH), the redshift obtained from Eq. (1). Table 1 also shows the values corresponding to ΔνNH) and –ΔH. When compared the hydrogen bond energies of 1-TE-BZT with those of other compounds [42], it can be concluded that hydrogen bonds in 1-TE-BZT are rather weak. Eventhough, the hydrogen bond-like interactions in 1-TE-BZT are the main factors contributing for the stabilisation of the 1H conformers, and the relative energies of 1H conformers can be mainly explained in terms of hydrogen bonds distances. However, other factors such as repulsions between negatively charged atoms or slight sterical hindrances (i.e.: the methyl group addressed to the SO₂ is a slightly destabilising factor if compared with the hydrogen atom) should also be considered.

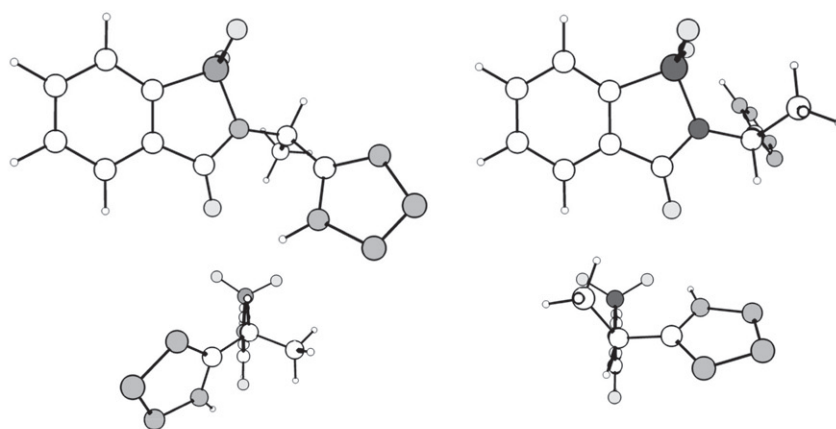
According to preliminary calculations (not presented) performed at a lower level of theory, all the barriers of interconversion between the 1H conformers were higher than 30 kJ mol⁻¹. Hence, considering the low relative energies between the three most stable 1H conformers and the high barriers of interconversion, these three forms can in principle be isolated experimentally in the argon matrices (note that due to the higher relative energy, 1H_GSk form does not have experimental relevance).

As explained in the previous paragraph, none of the conformers of 2H tautomer bears hydrogen bonds-like interactions. The position of H₂₈ in the tetrazole ring (2H position), oriented to the opposite side of the benzisothiazole ring precludes the formation of these stabilising forces, thus explaining the higher relative energies of 2H conformers and consequently, their non-experimental relevance.

3.3. Infrared spectra of the matrix-isolated compound

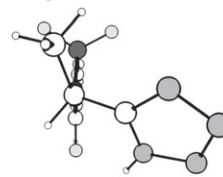
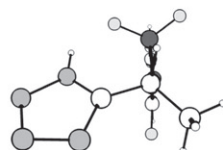
1-TE-BZT has 78 fundamental vibrations, all active in the infrared. The infrared spectrum of 1-TE-BZT isolated in an argon matrix with the substrate kept at 15 K during the matrix deposition is presented in Fig. 4, together with the calculated spectrum of the 1H_GSk' form. It must be considered that 1-TE-BZT is a molecule composed of 28 atoms, 16 of them belonging to the rigid benzisothiazole ring. This explains the reason why the bands corresponding to this ring are in general highly overlapped for the different 1H conformers, with the exception of the infrared modes relative to the oxygen atoms, for which the position strongly depend on the strength of the hydrogen bonds they establish. This fact makes especially difficult the assignment of bands to each of the most stable conformers. For this reason, we decided to simplify the

Tautomer 1H



1H_G'Sk'
0.00 kJ mol⁻¹
(-66.0°; -129.0°)

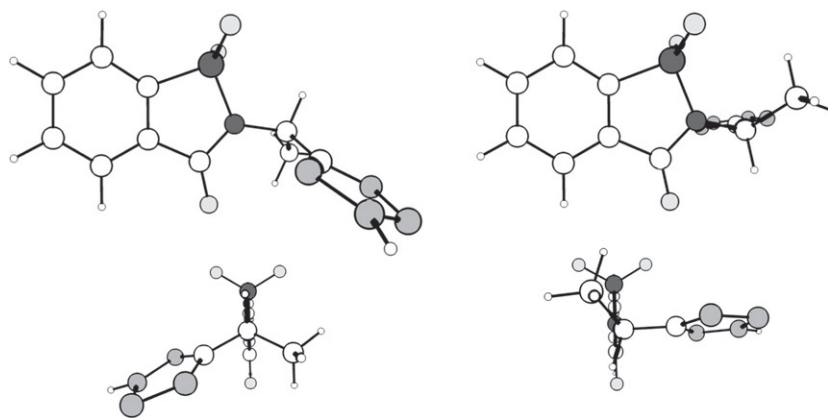
1H_GSk'
2.59 kJ mol⁻¹
(92.5°; -142.9°)



1H_G'Sk
4.25 kJ mol⁻¹
(-71.1°; 135.3°)

1H_GSk
8.30 kJ mol⁻¹
(73.7°; 118.8°)

Tautomer 2H



2H_G'G'
7.12 kJ mol⁻¹
(-63.1°; -16.8°)

2H_GG'
8.60 kJ mol⁻¹
(89.1°; -22.8°)

Fig. 3. DFT(B3LYP)/6-311++G(3pd,3df) optimised structures of the conformers of 1-TE-BZT. Two perspectives are provided, one with the viewpoint placed above the ring and the other with the viewpoint along the major axis of the molecule. The C₉–N₈–C₁₇–C₂₃ and N₈–C₁₇–C₂₃–N₂₄ dihedral angles are indicated in parentheses and zero point corrected relative energies are also shown.

assignments of bands in the freshly deposited matrix and, considering the nice fitting of the calculated 1H_GSk' spectrum with the

deposited compound in an argon matrix we performed the assignment of experimental bands to this low energy form (Table 2). In

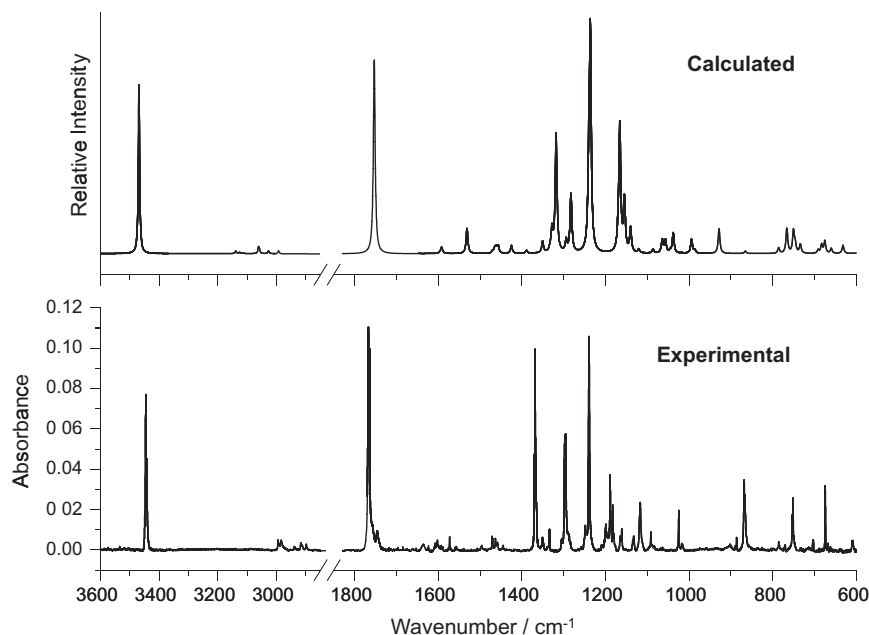


Fig. 4. Experimental infrared spectra (3600–600 cm^{-1} spectral range) of 1-TE-BZT in argon matrix (15 K), and DFT(B3LYP)/6-311++G(3pd,3df) calculated spectrum for conformer (*1H_GSk'*). The calculated spectrum was simulated using Lorentzian functions with full width at half maximum of 5 cm^{-1} with wavenumbers being scaled by 0.978.

agreement with the estimations reported in Section 3.2, the experimental observation of the νNH band at frequencies higher than 3400 cm^{-1} (Table 2) also indicates that the hydrogen bond-like interaction is relatively weak.

It must be underlined that the conformation of 1-TE-BZT as reagent does not influence the nature of the photoproducts observed after irradiation. Table S2 provides the complete set of frequencies of all the 1-TE-BZT isomers.

3.4. UV-irradiation experiments

The photochemistry of different matrix isolated benzothiazoles and tetrazoles has been addressed by our groups. Photodecomposition of tetrazoles involves cleavage of the tetrazolyl ring, leading to a variety of photoproducts, including azides, isocyanates or aziridines. The photochemistry of tetrazoles was also shown to be influenced by the chemical nature and conformational flexibility of substituents linked to the heterocycle, which may favour or exclude certain reaction channels, and also determine the relative amount of the final photoproducts [15–21].

In order to investigate the photochemical decomposition, the as-deposited compound was irradiated with UV light as described in Section 2.2 (Infrared spectroscopy and photochemical experiments). The wavelength used for irradiation has been chosen on the basis of the UV–Vis spectrum of 1-TE-BZT, which shows two absorption maxima at 275 and 385 nm (see in Fig. S1, the UV–Visible spectra of the compound in ethanol solution at room temperature). Irradiation at 385 nm did not stimulate any photofragmentation. After each irradiation, the sample was monitored by recording its infrared spectrum.

Irradiation at 275 nm induces a prompt decrease of the 1-TE-BZT bands with a concomitant observation of other new bands corresponding to the photoproducted species. Fig. 5 shows the spectroscopic results, obtained by subtracting the spectrum of the as-deposited matrix from the spectrum of the matrix irradiated during 40 min with laser ($\lambda = 275 \text{ nm}$), when almost all reagent was consumed. In Fig. 5, negative bands correspond to the

consumed reagent (1-TE-BZT) and the positive ones, to the photoproducts.

The calculated spectra for *1H_GSk'* and those of the photoproducts are also shown for comparison. A schematic summary of the observed photoprocesses is given in Fig. 6. The following photochemical pathways are proposed: (a) N_2 extrusion with the concomitant production of 2-[1-(1H-diaziren-3-yl)ethyl]-1,2-benzisothiazol-3(2H)-one 1,1-dioxide (BZT-DZ); (b) production of azide (N_3H) and 2-(1,1-dioxido-3-oxo-1,2-benzisothiazol-2(3H-yl)propanenitrile (BZTC $\equiv\text{N}$); (c) decarbonylation and ejection of azide (N_3H) to give 7-thia-8-azabicyclo[4.2.0] octa-1,3,5-triene 7,7 dioxide (TAOTD) and propene–nitrile. The complete assignment of the bands observed for the different photoproducts is given in Table 3, together with available previously reported values for the isolated compounds [43–45] and calculated data.

In Pathway (a), 1-TE-BZT ejects molecular nitrogen to give BZT-DZ. The ejection of molecular nitrogen is a common photodecomposition pathway in tetrazoles isolated in rare gas matrices [15–21]. BZT-DZ has two rotational axes [$\text{N}-\text{C}$, and $\text{C}-\text{C}(\text{N}_2\text{H})$] that can give rise to at least six different conformers (I, II, III, IV, V, VI), all of them with relative energies below 1.14 kJ mol^{-1} (Table S3). The most distinctive bands of this photoproduct could be identified in the irradiated matrices. As mentioned before for 1-TE-BZT, also in BZT-DZ, 16 out of 26 atoms belong to the benzothiazole ring. This means that 42 out of 72 vibrational modes are related with this ring. This fact explains the high overlap of bands corresponding to the different conformers of BZT-DZ, and also the overlap with bands corresponding to BZTC $\equiv\text{N}$ [produced in Pathway (b)]. However, the observation of some bands in relatively clean regions, such as those corresponding to $\nu(\text{N}=\text{N})$ of conformers I and V, at 1822 and 1803 cm^{-1} provides evidence for the photoproduction of BZT-DZ. Note also that the most intense band of the BZT-DZ is that of $\nu(\text{C}=\text{O})$ vibrational mode. This band fits nicely the calculated spectrum and represents another proof of the presence of BZT-DZ in the irradiated matrix. However, the low intensity of the $\nu(\text{C}=\text{O})$ experimental band indicates that Pathway (a) is not a major photodecomposition pathway of 1-TE-BZT. The assignment of the most relevant bands corresponding to this photoproduct is

Table 2

Experimental and calculated [B3LYP/6-311++G(3df,3pd); scaled by 0.978] vibrational frequencies (ν ; cm^{-1}) and calculated IR intensities (I , km mol^{-1}) for the 1H_GSK' form of 1 TE-BZT isolated in argon matrix.^a

Approximate description	Calculated 1H_GSK'		Observed ^b
	ν	I	
$\nu(\text{N-H})$	3468.5	262.6	3449.1/3445.6/3442.2
$\nu(\text{C-H})\text{ph}$	3138.8	4.2	2995.3/2984.7
$\nu(\text{C-H})\text{ph}$	3135.8	0.1	2939.2/2917.2
$\nu(\text{C-H})\text{ph}$	3125.0	2.2	2913.0/2899.5
$\nu(\text{C-H})\text{ph}$	3112.9	1.3	
$\nu(\text{CH}_3)\text{as}''$	3061.3	8.1	
$\nu(\text{CH}_3)\text{as}'$	3058.8	5.8	
$\nu(\text{CH}_{18})$	3027.3	4.3	
$\nu(\text{CH}_3)\text{s}$	2983.8	5.0	
$\nu(\text{C=O})$	1753.6	302.4	1766.9/1764.4
$\nu(\text{CC})\text{ph}$	1595.3	1.7	1602.0
$\nu(\text{CC})\text{ph}$	1591.6	9.6	1593.2
$\delta(\text{N-H}) + \nu(\text{C}_{17}-\text{C}_{23})$	1531.1	39.2	1573.1
$\gamma(\text{CH}_3)''$	1470.1	3.5	1496.2
$\delta(\text{C-H})\text{ph}$	1464.4	8.0	1471.4/1470.3
$\delta(\text{CH}_3)\text{as}''$	1461.0	7.3	1469.6
$\delta(\text{C-H})\text{ph}$	1456.5	10.9	
$\text{sci}(\text{C}_{23}-\text{C}_{17}-\text{H}_{18})$	1424.9	12.3	1463.4/1458.8
$\delta(\text{CH}_3)\text{s}$	1388.9	4.4	1445.0
$\delta(\text{N-H}) + \nu(\text{NN})\text{t} + \delta(\text{C-H}_{18})$	1350.5	18.0	1351.0
$\delta(\text{C-H}_{18})'' + \nu(\text{CC})\text{ph} + \delta(\text{N-H})$	1332.7	4.0	1334.0
$\delta(\text{C-H}_{18}) + \nu(\text{CC})\text{ph}$	1328.0	34.2	1370.8
$\nu(\text{SO}_2)\text{as}$	1318.1	185.1	1368.4/1361.4
$\delta(\text{C-H}_{18})'$	1294.1	18.2	1304.5
$\nu(\text{CC})\text{ph}$	1282.6	91.0	1297.2/1295.5
$\nu(\text{NN})\text{t} + \delta(\text{N-H})$	1239.9	106.9	1248.1/1245.2/1239.1
$\delta(\text{C-H})\text{ph} + \nu(\text{C}_2-\text{C}_9) + \nu(\text{C}_9-\text{N}_8)$	1236.3	329.2	
$\delta(\text{C-H})\text{ph} + \nu(\text{N}_8-\text{C}_{17})$	1169.6	20.9	1199.0/1189.1/1187.0
$\nu(\text{SO}_2)\text{s} + \delta(\text{C-H})\text{ph}$	1165.8	197.0	
$\delta(\text{C-H})\text{ph} + \nu(\text{SO}_2)\text{s}$	1154.7	81.1	1183.0/1180.6
$\delta(\text{CH}_3)\text{as}'$	1140.2	37.9	1165.1/1161.3
$\delta(\text{CH}_3)\text{as}''$	1120.4	5.7	1152.0
$\delta(\text{CH}_3)\text{as}''' + \delta(\text{NNN})$	1086.3	6.2	n.o.
$\nu(\text{NN})\text{t} + \delta(\text{NNN})\text{t}$	1064.4	20.7	1135.0/1132.6
$\nu(\text{NN})\text{t} + \delta(\text{CH}_3)\text{as}'''$	1056.6	20.2	1117.0
$\delta(\text{C-C})\text{ph}$	1045.9	3.3	n.o.
$\nu(\text{NN})\text{t}$	1038.2	31.7	1091.4
$\delta(\text{C-C})\text{ph}$	1017.8	0.8	n.o.
$\gamma(\text{C-H})\text{ph}$	1003.3	0.0	n.o.
$\gamma(\text{CH}_3)'$	994.3	21.9	1025.0
$\nu(\text{NN})\text{t}$	986.4	5.2	1016.5
$\gamma(\text{C-H})\text{ph}$	968.4	0.4	n.o.
$\delta(\text{C}_{17}\text{C}_{19}\text{C}_{23}\text{H}_{18})$	928.5	38.4	868.6/867.1
$\gamma(\text{C-H})\text{ph}$	886.9	0.2	n.o.
δ Skeletal	865.6	3.8	835.1
$\gamma(\text{CH})\text{ph}$	785.9	8.4	786.0
$\gamma(\text{N-H}_{28})$	766.3	38.3	753.9
$\gamma(\text{C-H})\text{ph}$	750.4	34.1	751.9
$\gamma(\text{NN})\text{t}$	746.2	13.0	749.3
$\delta(\text{CC})\text{ph}$	734.0	13.8	733.4/727.7
$\delta(\text{CC})\text{ph} + \nu(\text{CS})$	691.4	5.2	704.3/703.3
$\gamma(\text{NH}_{28}) + \gamma(\text{NN})\text{t}$	683.1	13.4	674.3
δ Skeletal	675.4	18.9	
δ Skeletal	660.0	7.7	663.0
δ Skeletal	632.0	12.7	611.2/608.8
$\gamma(\text{SO}_2)$	573.2	52.6	592.7
$\omega(\text{SO}_2)$	534.8	38.0	533.6
τ Skeletal	526.7	41.8	524.4
δ Skeletal	497.5	14.7	508.7

^a ν , stretching, δ , bending, γ , rocking, τ , torsion, ω , wagging, sci , scissoring, s , symmetric, as , anti-symmetric, t , tetrazole ring, n.o. , not observed. The infrared region below 500 cm^{-1} was not investigated; extensively delocalised modes are designated generally as skeletal bending (δ skeletal). See Fig. 2 for atom numbering.

also shown in Table 3. Due to the high overlap of bands, the assignment of BZT-DZ has been performed only on the most stable form I. Only in the regions where a doubtless assignment could be made, other forms were also considered [i.e. $\nu(\text{C=N})$, $\nu(\text{C=O})$]. In Pathway (b), the most intense band of azide was observed in the irradiated spectrum: 2142 cm^{-1} : $\nu(\text{N=N=N})\text{as}$. This band was observed in the spectrum of azide isolated in argon matrix at 2140 cm^{-1} [43]. The presence of azide in the photolysed matrix is reinforced by

the observation of the band due to the $\delta(\text{N-H})$ mode at $ca. 1127 \text{ cm}^{-1}$. According to the literature [43], this band occurs at 1150 cm^{-1} in the argon isolated azide. The deviation in the observed azide $\delta(\text{N-H})$ band compared with the literature value for the sole matrix-isolated compound indicates that once produced from fragmentation of 1-TE-BZT, azide interacts in the same matrix cage with the other compounds produced in this path (BZTC \equiv N) and in Pathway (c), where azide is also produced. The

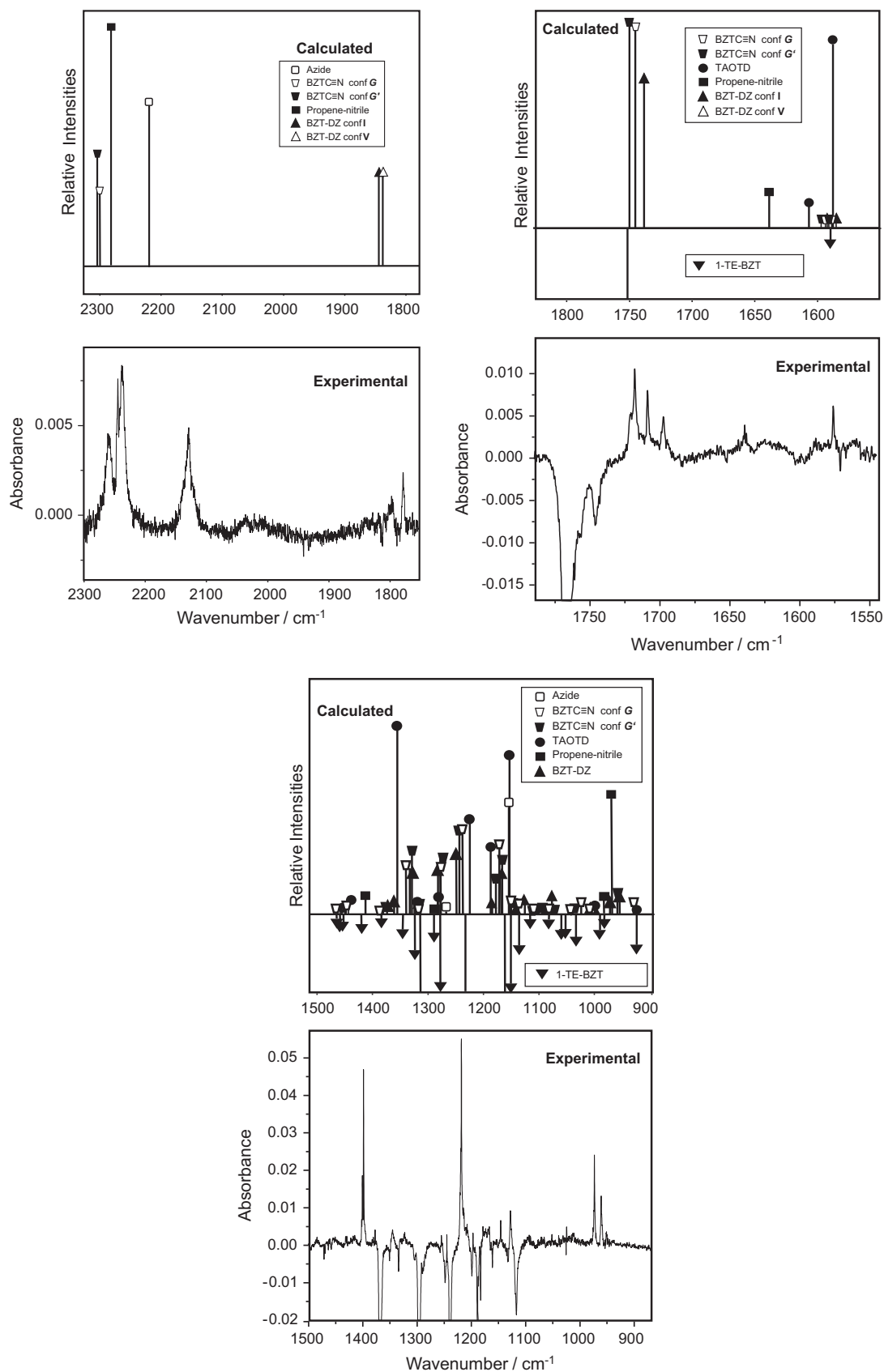


Fig. 5. (Bottom) Infrared difference spectrum [(irradiated matrix by UV light; $\lambda = 275$ nm; 40 min) minus (as-deposited matrix spectrum)] of 1-TE-BTZ in an argon matrix. Assignments for the bands due to photoproducts (pointing up) are given in Table 3. (Top) Simulation of the infrared difference spectrum shown in the bottom panel of the figure, based on the DFT(B3LYP)/6-311++G(3pd,3df) calculated spectra for 1-TE-BTZ ($1H_{GSK}$; bands pointing down) and for its photoproducts [Azide, BZTC \equiv N (conformer G and conformer G'), TAOTD, propene-nitrile and BZT-DZ (conformer I and V)]. The intensities of the individual spectra were multiplied by different factors to obtain a better simulation of the experimental difference spectra.

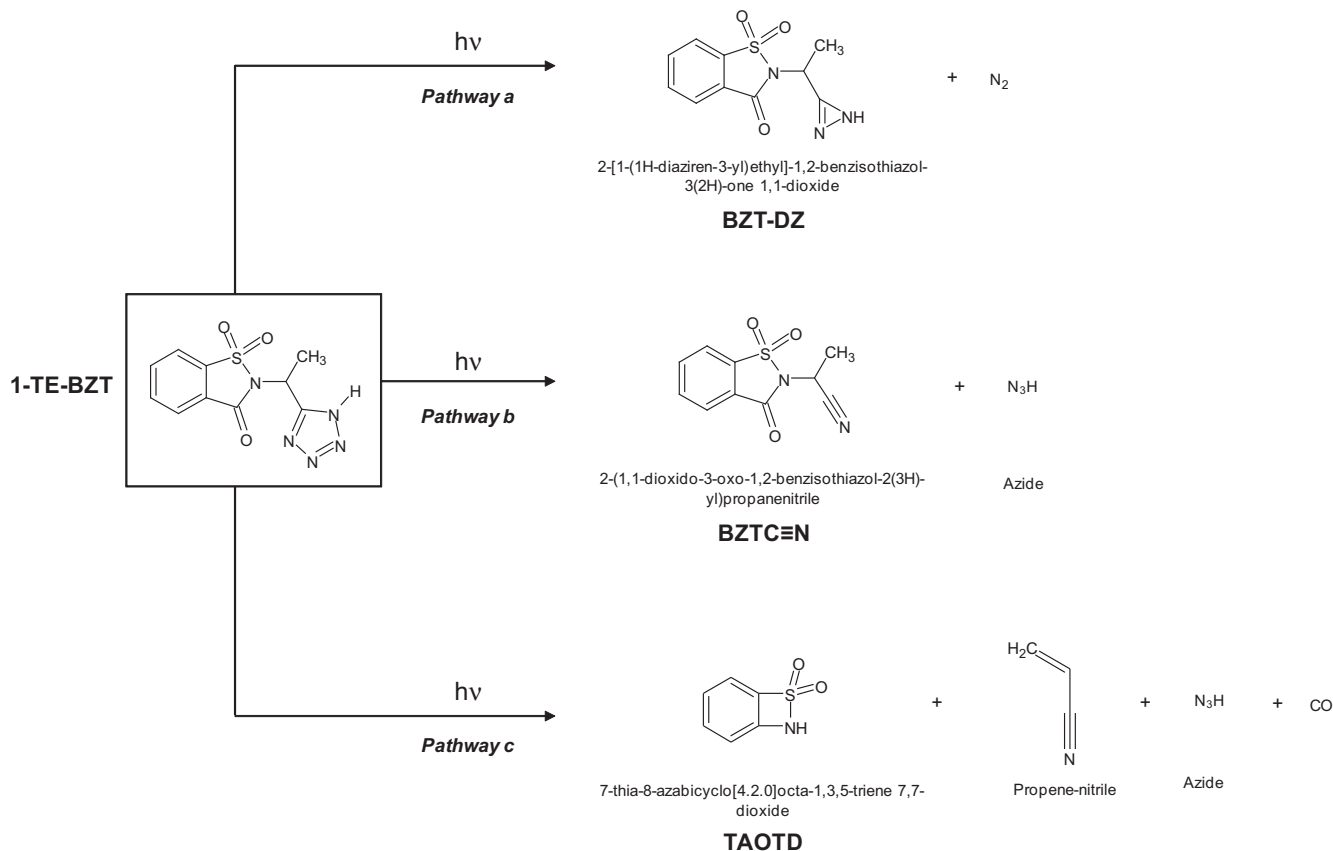


Fig. 6. Proposed reaction pathways resulting from irradiation of 1-TE-BZT monomer isolated in argon matrix.

hydrogen bonds connecting the different complexes, explain the shift of the $\delta(N-H)$ vibrational mode with regard to the matrix isolated pure azide.

The other photoproduct obtained in Pathway (b) is BZTC≡N. According to calculations at the DFT(B3LYP)/6-311++G(3df,3pd) level, only two conformers were found to correspond to minima structures. They differ in the orientation of the CNCC dihedral angle: G (CNCC = 91.7) and G' (CNCC = -59.5). Their energies are very close (the relative energies of G and G' forms are 0 and 0.07 kJ mol^{-1} , respectively) and the barrier of interconversion is ca. 20 kJ mol^{-1} . The bands at 2248 and 2241 cm^{-1} can be assigned to the $\nu(C\equiv N)$ vibrational mode of these two conformers (Fig. 5 and Table 3). Note that the low experimental intensity of bands intrinsically strong [i.e. $\nu(C=O)$, $\nu(S=O)$ symmetric and asymmetric], indicates that Pathway (b) is neither a major photodecomposition Pathway.

In Pathway (c), 1-TE-BZT decarbonylates to give TAOTD, propene-nitrile and azide. The carbon monoxide band is typically observed at 2138 cm^{-1} in argon matrices and in this case is overlapped with the $\nu(N=N=N)$ as band of azide, produced in Pathway (b) and also in this Pathway. The available information about propene-nitrile isolated in argon matrices [44] and calculations at the DFT(B3LYP)/6-311++G(3df,3pd) level of theory aided the confirmation of propene-nitrile in the photolysed matrix (see for example experimental bands at 975 and 973 cm^{-1} , ascribed to the $\omega(CH_2)$ vibrational mode. The opening of the benzisothiazole ring gives TAOTD. The most intense bands of this compound occur in the 1400–950 cm^{-1} range and fit nicely the calculated spectrum. The experimental intensity of the bands corresponding to the photoproducts generated in Pathway (c) is higher than that of the photoproducts of Pathways (a) and (b). This fact is particularly

evident in the carbonyl region, where only products from (a) and (b) are observed. In the region 1400–950 cm^{-1} , photoproducts obtained in all the three pathways are observed. However, the most intense bands observed in this region in the photolysed matrices can be ascribed to photoproducts of Pathway (c) (Fig. 5 and Table 3). This fact allows us to consider this pathway as the preferred photodecomposition channel for 1-TE-BZT.

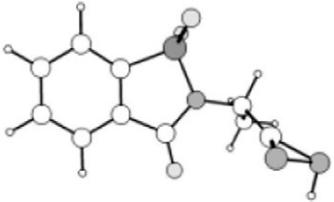
4. Conclusions

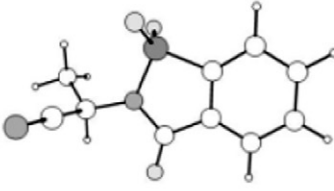
In this work, the alkyl-linked saccharyl-tetrazole conjugate 1-TE-BZT has been synthesised and studied from the view point of its molecular structure and vibrational spectra using matrix isolation FTIR spectroscopy. All experimental results have been supported by quantum chemical calculations at a high level of theory [DFT(B3LYP)/6-311++G(3df,3pd)].

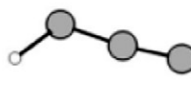
In 1-TE-BZT, the hydrogen atom bound to the tetrazole ring gives rise to two different tautomers, 1H and 2H. In addition, the two rotational axes of 1-TE-BZT can give rise to different conformational isomers within each tautomeric form. As a whole, the theoretical calculations led to the identification of four conformers 1H and two conformers 2H. The experimental spectrum obtained from the as deposited compound could be assigned to conformer 1H_GSK'.

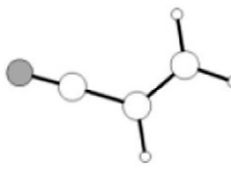
The photochemistry of the saccharyl-tetrazole conjugate 1-TE-BZT has also been addressed. However, the complexity of the studied compound makes difficult the analysis of the experimental information, the interpretations not being conclusive. In this context, considering the high reactivity of the tetrazole ring and the photostability of the benzisothiazole moiety, three photolysis pathways were proposed to interpret the photodecomposition

Table 3
Experimental and calculated [B3LYP/6-311++G(3df,3pd); scaled by 0.978] vibrational frequencies (ν ; cm^{-1}) and calculated IR intensities (I , km mol^{-1}) for the observed photoproducts of 1-TE BZT monomer isolated in argon matrix.^a

Approximate Description	Sym	Conformer	Observed	Calculated		Literature Data							
			ν	ν	I	ν	Ref						
TAOTD	C1												
								$\nu(\text{C-C})_{\text{ph}}$	A	1578	1589.2	40.6	
								$\delta(\text{C-H})_{\text{ph}}$	A	1432/1430	1446.7	18.8	
								$\nu(\text{SO}_2)_{\text{as}}$	A	1402 / 1400 / 1399	1358.9	213.8	
								$\delta(\text{C-H})_{\text{ph}}$	A	1323	1328.7	15.2	
								$\delta(\text{C-H})_{\text{ph}}$	A	1128	1157.2	50.1	
								$\nu(\text{SO}_2)_{\text{s}}$	A		1156.4	133.4	
								$\delta(\text{C-H})_{\text{ph}}$	A	800	755.8	90.2	
								$\delta(\text{C-H})_{\text{ph}}$	A	768	738.7	29.0	
								$\gamma(\text{N-H})$	A	631	628.7	109.0	
								$\gamma(\text{SO}_2)$	A	607	598.2	61.9	
								$\omega(\text{SO}_2)$	A	553	544.9	57.4	
BZT-DZ	C1												
								$\nu(\text{C=N})$	A	I	1822	1845.2	18.7
										V	1803	1839.3	19.1
								$\nu(\text{C=O})$	A	I	1709	1741.4	294.3
										V	1698	1737.2	328.8
								$\nu(\text{SO}_2)_{\text{as}}$	A	I	1377	1338.7	182.8
								$\delta(\text{C-H})_{\text{ph}}$	A	I	1326	1328.8	15.0
								$\delta(\text{N-H})$	A			1324.5	21.7
								$\delta(\text{C-H})_{\text{ph}}$	A	I	1292	1288.4	104.5
												1286.6	87.6
								$\delta(\text{C-H})_{\text{ph}}$	A	I	1255	1254.8	217.3
								$\delta(\text{C-H})_{\text{ph}}$	A	I	1197	1189.8	50.6
								$\nu(\text{SO}_2)_{\text{s}}$	A	I	1167	1175.0	174.3
								$\delta(\text{C-H})_{\text{ph}}$	A	I	1146	1160.0	29.4
								$\delta(\text{N-H})$	A	I	976	978.2	23.1
								$\nu(\text{N-C})$	A	I	959 (sh)	960.4	57.6
								$\gamma(\text{CH})_{\text{ph}}$	A	I	803 (sh)	786.5	7.1
								$\gamma(\text{CH}_3)'$	A	I	803 (sh)	781.0	12.8
$\gamma(\text{C-H})_{\text{ph}}$	A	I	801 (sh) / 800	749.9	39.3								
$\delta(\text{C-C})_{\text{ph}}$	A	I	767 (sh)	733.7	9.4								
C_4 ph out of plane	A	I	662	674.3	24.6								

BZTC≡N		C1				
$\nu(\text{C-N})$	A	G' G	2263	{ 2306.0 2302.5	{ 0.8 0.6	
$\nu\text{C=O}$	A	G' G	1722 1718	1747.3 1745.3	298.9 333.6	
$\nu(\text{SO}_2)\text{as} + \delta(\text{N-C-H})$	A	G	1377	1344.8	148.9	
$\nu(\text{SO}_2)\text{as} + \delta(\text{N-C-H})$	A	G		1341.3	58.2	
$\nu(\text{SO}_2)\text{as}$	A	G'		1337.0	182.6	
$\delta(\text{C-H})\text{ph}$	A	G'	1255	1251.6	257.6	
	A	G	1245	1241.8	294.7	
$\nu(\text{SO}_2)\text{as}$	A	G G'	1145	1175.8	232.4	
		G'		1174.7	149.8	
$\omega(\text{SO}_2)$	A	G G'	575	568.7	42.2	
		G'		567.0	39.6	

Azide		Cs					
$\nu(\text{N=N=N})\text{as}$	A'		2139	2220.0	408.2	2140	[43]
$\delta(\text{N-H})$	A'		1128	1159.0	223.5	1150	[43]

Propene-nitrile		Cs					
$\nu(\text{C-C=N})\text{as}$	A'		2249 / 2242	2281.9	9.6		
$\nu(\text{C=C})$	A'		1639	1638.2	1.5		
$\delta(\text{CH}_2)\text{as}$	A'		1417 / 1415	1418.3	7.2		
$\omega(\text{CH=CH}_2)$	A''		973 / 960	974.8	48.2	974 / 968 / 956 / 954 / 953	[44]
$\gamma(\text{CH}_2) + \nu(\text{C-C})$	A'		856	863.1	1.6		
$\gamma(\text{C-C})$	A''		707	698.3	11.5		

Carbon monoxide				
$\nu(\text{C=O})$	A	2138	2138	[45]

^a Only the investigated bond are shown.

ν , stretching, δ , bending, γ , rocking, s, symmetric, as, anti-symmetric, ph, phenyl; sh, shoulder.

occurred upon matrix irradiation with UV $\lambda = 275$ nm: (a) ejection of molecular nitrogen to give at least six different conformers of BZT-DZ; (b) cleavage of the tetrazole ring to give azide and BZTC≡N, and (c) decarbonylation of 1-TE-BZT to give propene-nitrile, azide and TAOTD. The comparison of the relative intensities of the bands of the photoproducts obtained from the three channels allowed us to conclude that Pathway (c) is the preferred one.

Although with low efficiency, this was the first time that photocleavage of the benzothiazole ring in rare gas matrices

was observed. The pathway proposed opens up several possibilities in the interpretation of the molecular mechanisms leading to photodecomposition of such stable aromatic compounds. The fact that this particular saccharyl derivative is more prone to ring photocleavage than the ones that we previously attempted to photolyse, namely alkyl and allyl saccharyl ethers, may be ascribed to the powerful electron-withdrawing effect of the tetrazole substituent which deviates electron density from the ring, weakening the C—C bond to the carbonyl and subsequently favouring α

cleavage. We now aim at exploring further the photochemistry of benzisothiazoles.

Acknowledgements

The authors are grateful to Fundação para a Ciência e Tecnologia and FEDER (Projects PTDC/QUI/67674/2006 and PTDC/QUI/71203/2006), bilateral cooperation grant (FCT-MinCyT PO/09/18) and CYTED (Network 108RT0362) for financial support. A.G.Z. is member of the Research Career CONICET, Argentina. A.B., B.M.G. and L.D. acknowledge FCT for the award of postdoctoral and doctoral Grants (SFRH/BPD/66154/2009, SFRH/BPD/44689/2008 and SFRH/BD/62090/2009, respectively). We would also like to acknowledge the Milipeia Computer Centre (University of Coimbra), research project “Computação Avançada em Espectroscopia Molecular”.

Appendix A. Supplementary material

Supplementary data associated with this article can be found, in the online version, at <http://dx.doi.org/10.1016/j.molstruc.2012.04.081>.

References

- [1] Y. Tamura, F. Watanabe, T. Nakatani, K. Yasui, M. Fuji, T. Komurasaki, H. Tsuzuki, R. Maekawa, T. Yoshioka, K. Kawada, K. Sugita, M. Ohtani, *J. Med. Chem.* 41 (1998) 640.
- [2] H. Zhao, Z.-R. Qu, H.-Y. Ye, R.-G. Xiong, *Chem. Soc. Rev.* 37 (2008) 84.
- [3] E.J. Baran, V.T. Yilmaz, *Coord. Chem. Rev.* 250 (2006) 1980.
- [4] M.L.S. Cristiano, R.A.W. Johnstone, P.J. Price, *J. Chem. Soc. Perkin Trans. 1* (1996) 1453.
- [5] N.C.P. Araújo, A.F. Brigas, M.L.S. Cristiano, L.M.T. Frija, E.M.O. Guimarães, R.M.S. Loureiro, *J. Mol. Catal. A: Chem.* 215 (2004) 113.
- [6] L.M.T. Frija, M.L.S. Cristiano, E.M.O. Guimarães, N.C. Martins, R.M.S. Loureiro, J. Bikley, *J. Mol. Catal. A: Chem.* 242 (2005) 241.
- [7] R.A.W. Johnstone, A.H. Wilby, I.D. Entwistle, *Chem. Rev.* 85 (1985) 129.
- [8] J.V. Barkley, M.L.S. Cristiano, R.A.W. Johnstone, R.M.S. Loureiro, *Sect. C: Cryst. Struct. Commun.* 53 (1997) 383.
- [9] M.L.S. Cristiano, A.F. Brigas, R.A.W. Johnstone, R.M.S. Loureiro, P.C.A. Pena, *J. Chem. Res. (S)* (1999) 704.
- [10] N.C.P. Araújo, P.M.M. Barroca, J.F. Bickley, A.F. Brigas, M.L.S. Cristiano, R.A.W. Johnstone, R.M.S. Loureiro, P.C.A. Pena, *J. Chem. Soc. Perkin Trans. 1* (2002) 1213.
- [11] R. Almeida, A. Gómez-Zavaglia, A. Kaczor, M.L.S. Cristiano, M.E.S. Eusébio, T.M.R. Maria, R. Fausto, *Tetrahedron* 64 (2008) 3296.
- [12] A. Kaczor, L. Proniewicz, R. Almeida, A. Gómez-Zavaglia, M.L.S. Cristiano, A.M. Matos Beja, M. Ramos Silva, R. Fausto, *J. Mol. Struct.* 892 (2008) 343.
- [13] L.M.T. Frija, R. Fausto, R.M.S. Loureiro, M.L.S. Cristiano, *J. Mol. Catal. A: Chem.* 305 (2009) 142.
- [14] A. Gómez-Zavaglia, A. Ismael, L.L.L. Cabral, A. Kaczor, J.A. Paixão, R. Fausto, M.L.S. Cristiano, *J. Mol. Struct.* 1003 (2011) 103.
- [15] A. Gómez-Zavaglia, I.D. Reva, L.M.T. Frija, M.L.S. Cristiano, R. Fausto, *J. Phys. Chem. A* 109 (2005) 7967.
- [16] A. Gómez-Zavaglia, I.D. Reva, L.M.T. Frija, M.L.S. Cristiano, R. Fausto, *J. Photochem. Photobiol. A* 179 (2006) 243.
- [17] A. Gómez-Zavaglia, I.D. Reva, L.M.T. Frija, M.L.S. Cristiano, R. Fausto, *J. Mol. Struct.* 786 (2006) 182.
- [18] A. Gómez-Zavaglia, I.D. Reva, L.M.T. Frija, M.L.S. Cristiano, R. Fausto, *J. Photochem. Photobiol. A* 180 (2006) 175.
- [19] L.M.T. Frija, I.D. Reva, A. Gómez-Zavaglia, M.L.S. Cristiano, R. Fausto, *J. Phys. Chem. A* 111 (2007) 2879.
- [20] L.M.T. Frija, I.D. Reva, A. Gómez-Zavaglia, M.L.S. Cristiano, R. Fausto, *Photochem. Photobiol. Sci. (PPS)* 6 (2007) 1170.
- [21] A. Gómez-Zavaglia, I.D. Reva, L.M.T. Frija, M.L.S. Cristiano, R. Fausto, *Chem. Phys. Res. J.* 1 (2009) 221.
- [22] A. Ismael, M.L.S. Cristiano, R. Fausto, A. Gómez-Zavaglia, *J. Phys. Chem. A* 114 (2010) 13076.
- [23] I. Elghamry, D. Döpp, *Tetrahedron Lett.* 42 (2001) 5651.
- [24] D.W. Cho, S.W. Oh, D.U. Kim, H.J. Park, J.Y. Xue, U.C. Yoon, P.S. Mariano, *Bull. Korean Chem. Soc.* 31 (2010) 2453.
- [25] I. Elghamry, D. Döpp, G. Henkel, *Synthesis* 8 (2001) 1223.
- [26] D. Döpp, *Int. J. Photoenergy* 3 (2001) 41.
- [27] R. Krishnan, J.S. Binkley, R. Seeger, J.A. Pople, *J. Chem. Phys.* 72 (1980) 650.
- [28] A.D. McLean, G.S. Chandler, *J. Chem. Phys.* 72 (1980) 5639.
- [29] M.J. Frisch, J.A. Pople, J.S. Binkley, *J. Chem. Phys.* 80 (1984) 3265.
- [30] T. Clark, J. Chandrasekhar, G.W. Spitznagel, P.V.R. Schleyer, *J. Comput. Chem.* 4 (1983) 294.
- [31] P.M.W. Gill, B.G. Johnson, J.A. Pople, M.J. Frisch, *Chem. Phys. Lett.* 197 (1992) 499.
- [32] A.D. Becke, *Phys. Rev. A* 38 (1988) 3098.
- [33] C.T. Lee, W.T. Yang, R.G. Parr, *Phys. Rev. B* 37 (1988) 785.
- [34] P. Pulay, *J. Comput. Chem.* 3 (1982) 556.
- [35] GAMESS, version R1 (1-October-2010), M. Schmidt, K. Baldridge, J. Boatz, S.T. Elbert, M.S. Gordon, J.H. Jensen, S. Koseki, N. Matsunaga, K.A. Nguyen, S.J. Su, T.L. Windus, M. Dupuis, J. Montgomery, *J. Comput. Chem.* 14 (1993) 1347.
- [36] A. Gómez-Zavaglia, A. Kaczor, R. Almeida, M.L.S. Cristiano, M.E.S. Eusébio, T.M.R. Maria, P. Mobili, R. Fausto, *J. Phys. Chem. A* 113 (2009) 3517.
- [37] I.G. Binev, B.A. Stamboliyska, E.A. Velcheva, *Spectrosc. Acta Part A – Mol. Biomol. Spectrosc.* 52 (1996) 1135.
- [38] Y.I. Binev, C.T. Petkov, L. Pejov, *Spectrosc. Acta Part A – Mol. Biomol. Spectrosc.* 56 (2000) 1949.
- [39] P. Naumov, G. Jovanovski, *Struct. Chem.* 11 (2000) 19.
- [40] G. Jovanovski, S. Tanceva, B. Soptrajanov, *Spectrosc. Lett.* 28 (1995) 1095.
- [41] A. Kaczor, R. Almeida, A. Gomez-Zavaglia, M.L.S. Cristiano, R. Fausto, *J. Mol. Struct.* 876 (2008) 77.
- [42] M. Rozenberg, G. Shoham, I. Reva, R. Fausto, *Phys. Chem. Chem. Phys.* 7 (2005) 2376.
- [43] S. Shen, J.R. Durig, *J. Mol. Struct.* 661–662 (2003) 49.
- [44] W.O. George, E.N. Lewis, D.A. Williams, W.F. Maddams, *Appl. Spectrosc.* 36 (1982) 592.
- [45] F. Duvernay, T. Chiavassa, F. Borget, J.P. Aycard, *Chem. Phys.* 298 (2004) 241.